Supplementary Materials: Synthesis and Reactivity of Mn–CF_3 Complexes.

Alex L. Daniels, Jason G. Da Gama, Racquel Edjoc, Bulat M. Gabidullin and R. Tom Baker*

Details for X-ray Crystallography. For **3**, **6,** and **9**: samples were mounted on thin glass fibers using paraffin oil and were cooled to 200K prior to data collection. Data were collected on a Bruker AXS KAPPA single crystal diffractometer equipped with a sealed Mo tube source (wavelength 0.71073Å) APEX II CCD detector. Raw data collection and processing were performed with APEX II software package from BRUKER AXS.[ref] Diffraction data were collected with a sequence of 0.5° ω scans at 0, 90, 180, and 270° in φ. Initial unit cell parameters were determined from 60 data frames collected at different sections of the Ewald sphere. Semi-empirical absorption corrections based on equivalent reflections were applied. Systematic absences in the diffraction data set and unit-cell parameters were consistent with triclinic systems. Solutions in centrosymmetric space group yielded chemically reasonable and computationally stable results of refinement. The structures were solved by direct methods, completed with difference Fourier synthesis, and refined with full-matrix least-squares procedures based on F2. In the structure, compound molecules are situated in the general position. All non-hydrogen atoms were refined anisotropically with satisfactory thermal parameters values. Additional crystallographic data and selected data collection parameters are reported below. The cif files for the following structures are available as Supporting Information.

$Mn(CO)_3(Bipy)CF_3$ (3): Empirical Formula: $C_{14}H_8F_3MnN_2O_3$; FW = 364.16; Crystal size: 0.229 X 0.187 X 0.058 mm^3; Crystal System: Triclinic; Space Group: P_{-1}; Z = 2; a = 6.9984 (5) Å, b = 9.9870 (9) Å, c = 10.8023 (8), α = 88.652 (3)º, β = 71.277 (2)º, γ = 75.664 (2)º; Volume = 691.50 (0) $Å^3$; Calculated Density = 1.749 g/cm^3; Absorption Coefficient = 1.006 mm^{-1}; F(000) = 364.0; Θ range for data collection: 0.794 to 26.375º; Limiting indices: -8≤h≤8, -12≤k≤12, -13≤l≤13: Reflections collected/unique: 8801/8801; R(int) = ?; Completeness to Θ = 25.242: 100%; Max and min transmission: Data / Restraint / parameters: 8801 / 0 / 209; Goodness-of-fit on F^2: 1.048; Final R indices [I>2σ(I)]: R1 = 0.0846, wR2 = 0.1213 ; R indices (all data): R1 = 0.1574, wR2 = 0.1456; largest diff. peak/hole: 0.773 / -0.640 $eÅ^{-3}$.

$Mn(CO)_2(Tpy)CF_3$ (4): Empirical Formula: $C_{18}H_{11}F_3MnN_3O_2$; FW = 413.24; Crystal size: 0.11 X 0.05 X 0.03 mm^3; Crystal System: Monoclinic; Space Group: $P_{21/n}$; Z = 4; a = 9.0038 (3) Å, b = 13.9811 (5) Å, c = 13.4556 (5), α = 90.000(0)º, β = 107.861 (2)º, γ = 90.000 (0)º; Volume = 1612.20 (10) $Å^3$; Calculated Density = 1.702 g/cm^3; Absorption Coefficient = 4.890 mm^{-1}; F(000) = 832.0; Θ range for data collection: 0.746 to 56.026º; Limiting indices: -11≤h≤10, -17≤k≤16, -16≤l≤16: Reflections collected/unique: 16611/3133; R(int) = ?; Completeness to Θ = 25.242: 98.4%; Max and min transmission: Data / Restraint / parameters: 3133 / 0 / 245; Goodness-of-fit on F^2: 1.037; Final R indices [I>2σ(I)]: R1 = 0.0574, wR2 = 0.1272 ; R indices (all data): R1 = 0.0893, wR2 = 0.1467; largest diff. peak/hole: 0.54 / -0.61 $eÅ^{-3}$.

$Mn(Phen)_2(OTf)_2$ (9): Empirical Formula: $C_{26}H_{16}F_6MnN_4O_6S_2$; FW = 713.49; Crystal size**:** 0.17 X 0.11 X 0.08 mm^3; Crystal System: Monoclinic; Space Group: $C_{2/c}$; Z = 4; a = 9.7736 (4) Å, b = 14.3565 (7) Å, c = 19.9052 (9), α = 90.000 (0)º, β = 95.585 (2)º, γ = 90.000 (0)º; Volume = 2779.70 (2) $Å^3$; Calculated Density = 1.705 g/cm^3; Absorption Coefficient = 4.115 mm^{-1}; F(000) = 1436.0; Θ range for data collection: 0.379 to 60.646º; Limiting indices: -12≤h≤12, -18≤k≤18, -25≤l≤25: Reflections collected/unique: 20729/3208; R(int) = 0.0279; Completeness to Θ = 60.646: 100%; Max and min transmission: Data / Restraint / parameters: 3208/ 0/ 205; Goodness-of-fit on F^2: 1.102; Final R indices [I>2σ(I)]: R1 = 0.0357, wR2 = 0.0944 ; R indices (all data): R1 = 0.0366, wR2 = 0.0944; largest diff. peak/hole: 0.50 / -0.55 $eÅ^{-3}$.

IR Spectra:

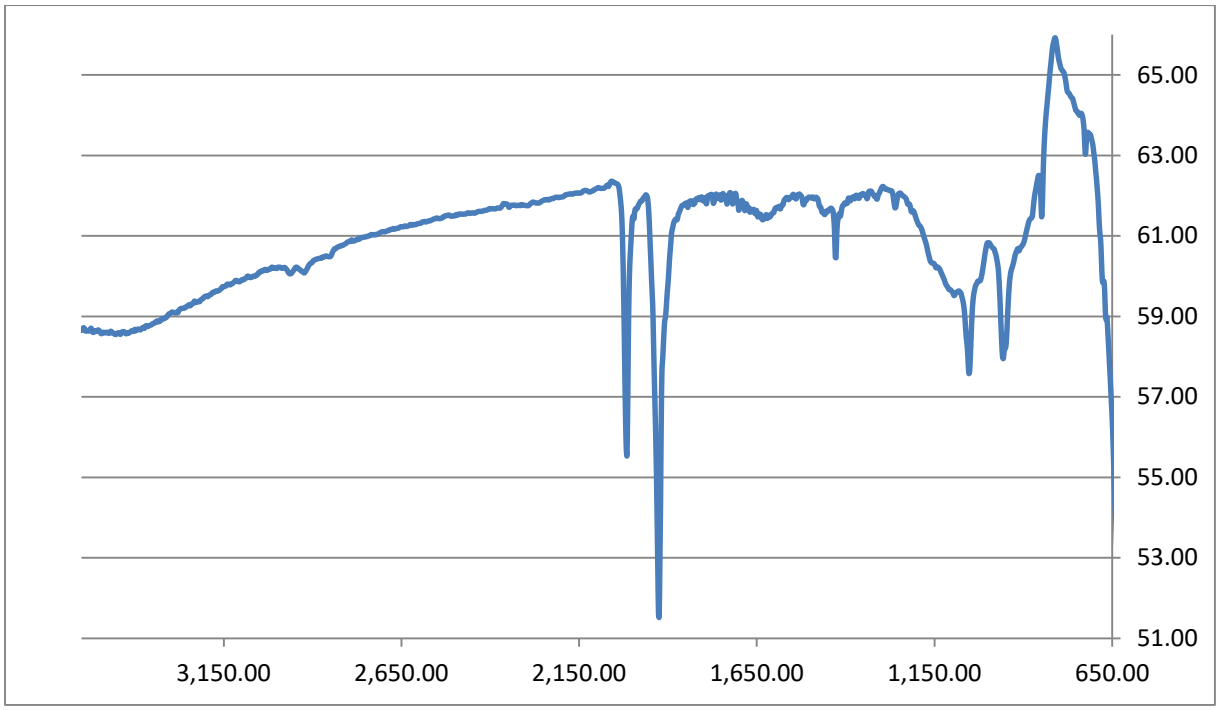

Figure S1: FT-IR spectra (Nicolet Nexus 670 instrument, neat/solid samples) for $Mn(CO)_2(Phen)CF_3$ (**1**)

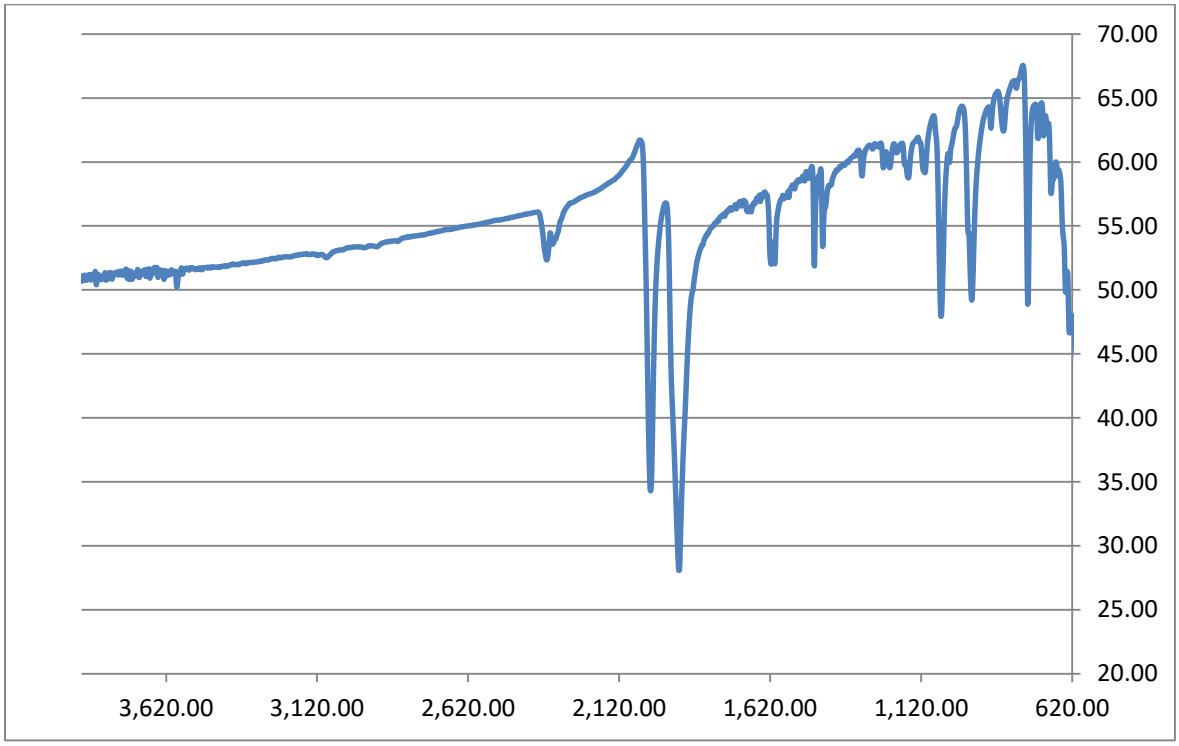

Figure S2: FT-IR spectra (Nicolet Nexus 670 instrument, neat/solid samples) for $Mn(CO)_3(Bipy)CF_3$ (**2**).

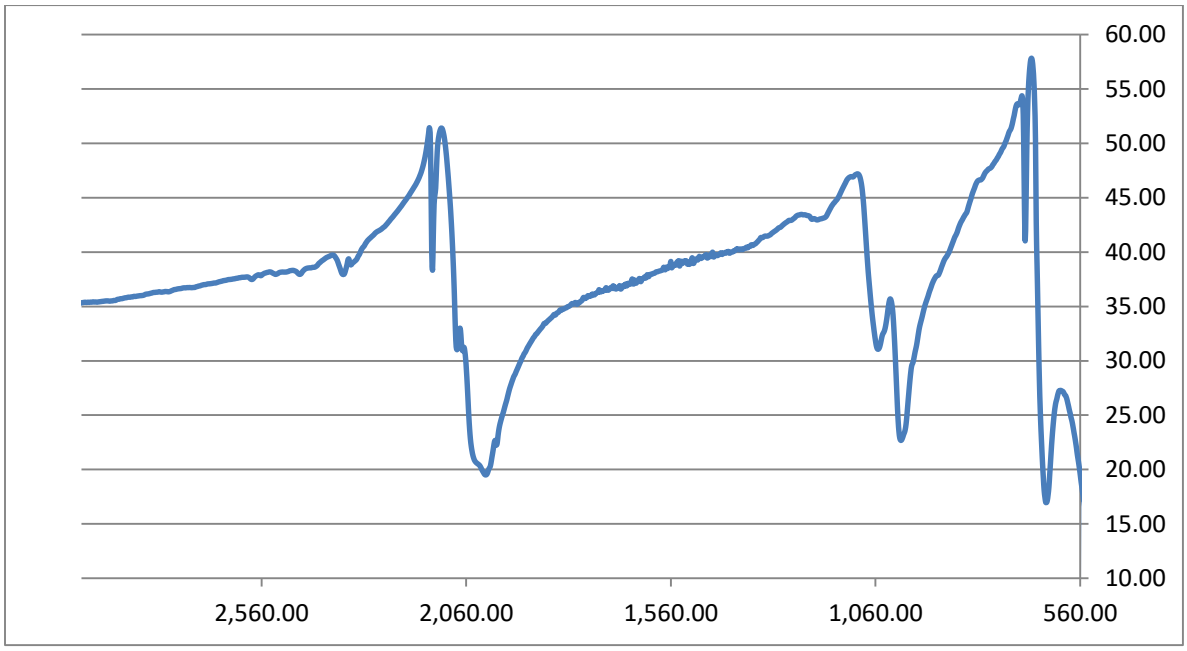

Figure S3: FT-IR spectra (Nicolet Nexus 670 instrument, neat/solid samples) for $Mn(CO)_5CF_3$.

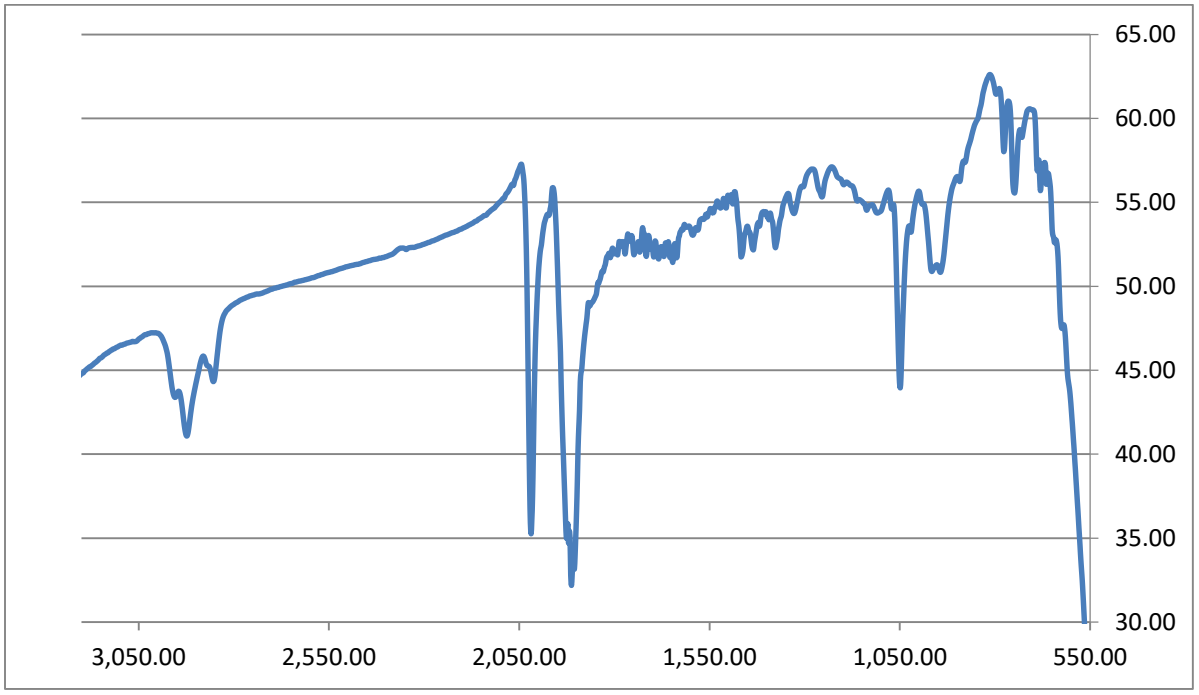

Figure S4: FT-IR spectra (Nicolet Nexus 670 instrument, neat/solid samples) for $Mn(CO)_2(NNS)CF_3$ (**4**)

NMR Spectra:

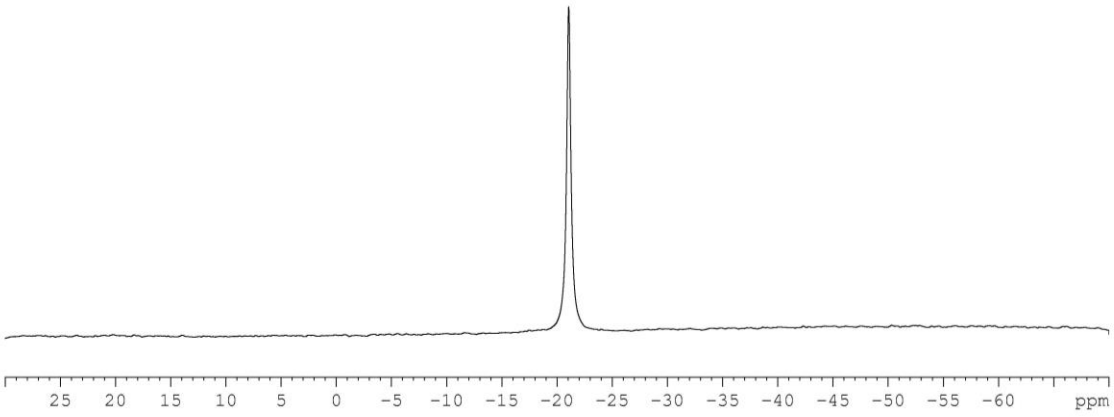

Figure S5: ^{19}F NMR (282 Mhz, CD_3CN) spectrum of complex **3**.

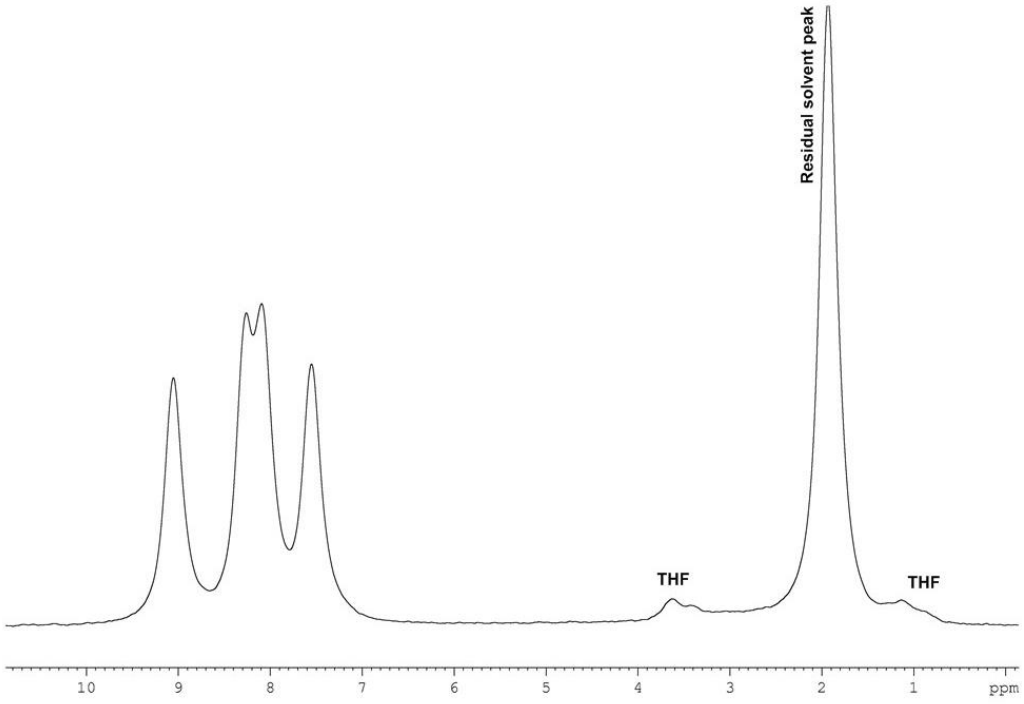

Figure S6: ^{1}H NMR (300 Mhz, CD_3CN) of complex **3.**

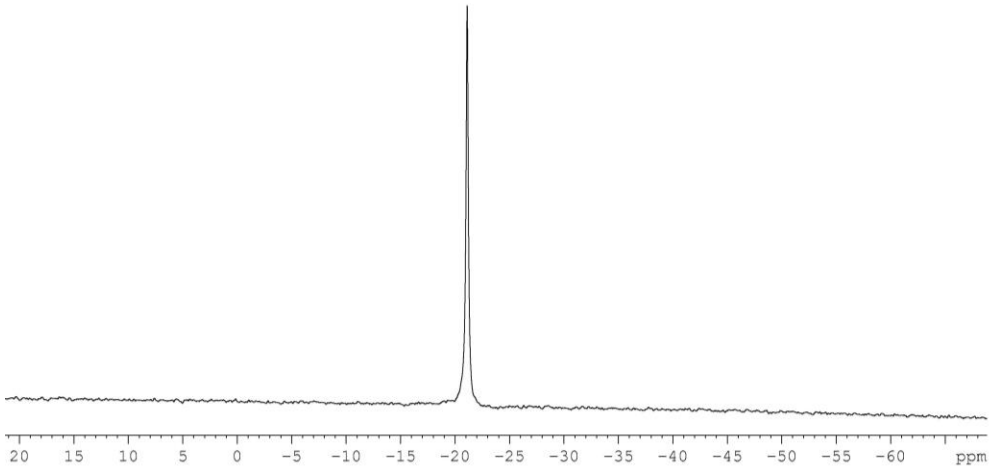

Figure S7: ^{19}F NMR (282 Mhz, $CDCl_3$) of complex **4.**

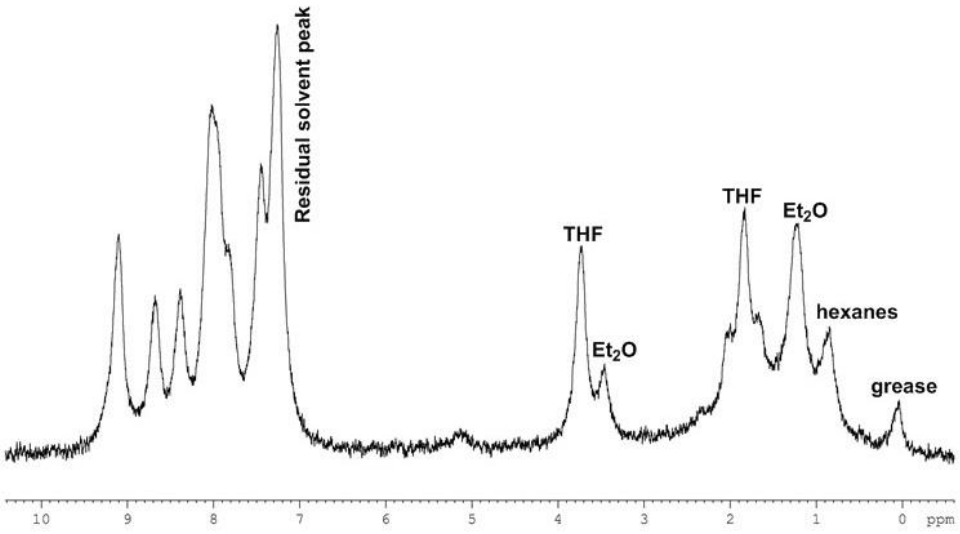

Figure S8: ^{1}H NMR (300 Mhz, $CDCl_3$) of complex **4.**

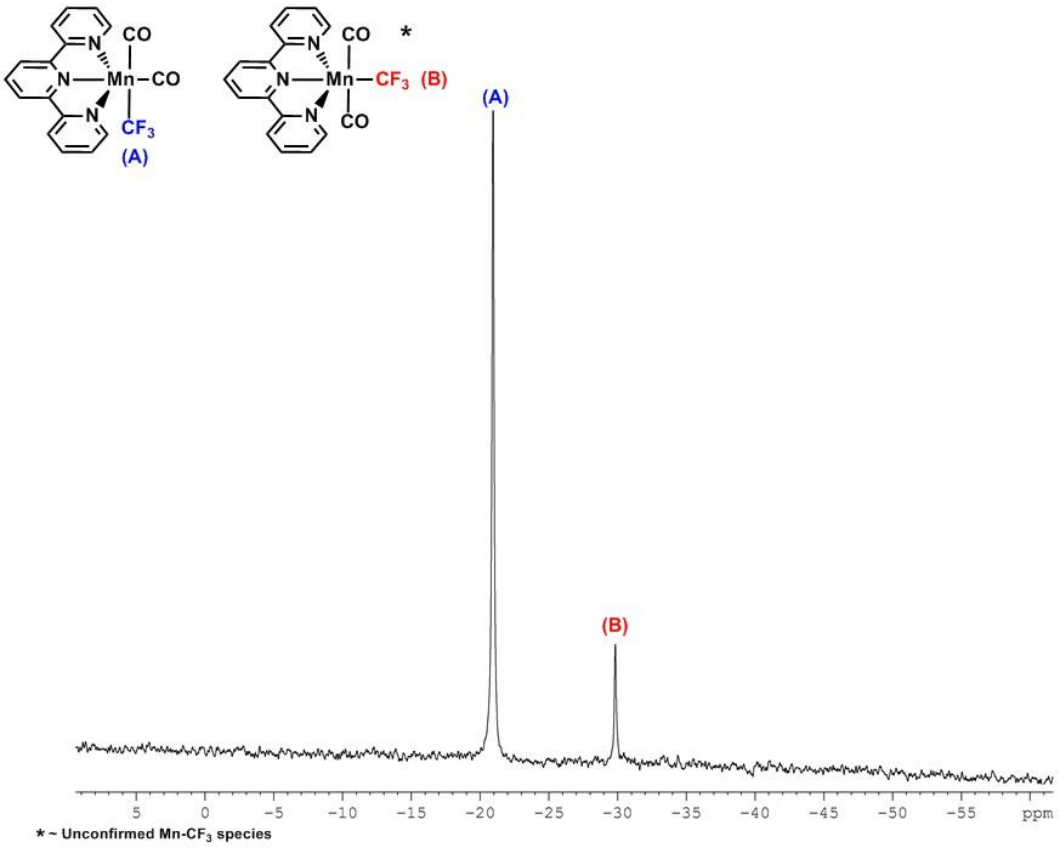

Figure S9: ^{19}F NMR (282 MHz, CD_3CN) spectrum of complex **6**. Spectrum shows a minor Mn-CF_3 peak which is proposed to be the trans-Mn-CF_3 product.

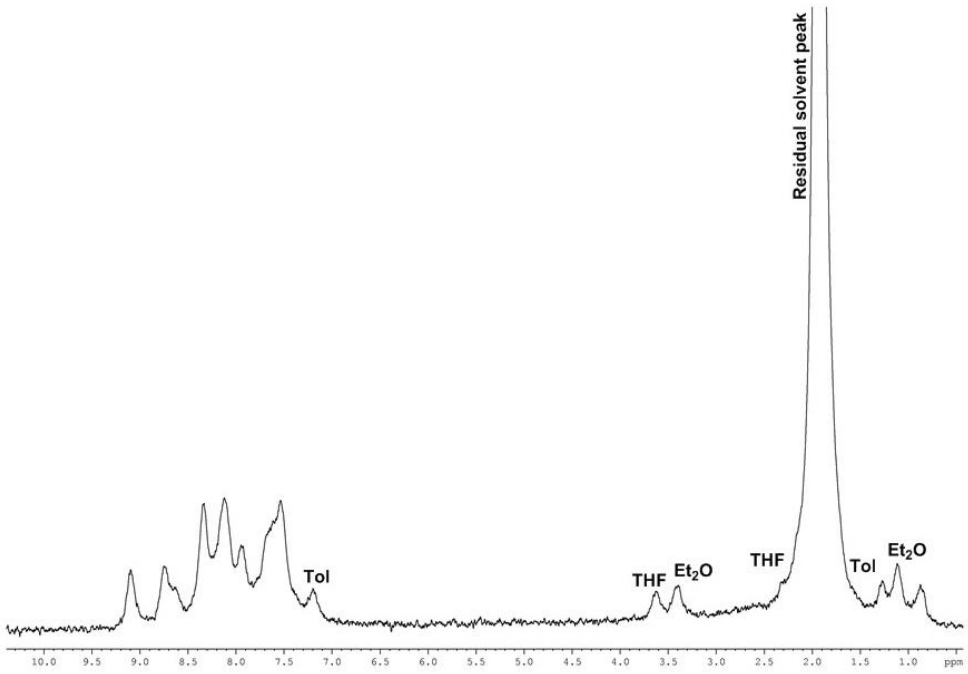

Figure S10: ^{1}H NMR (300 MHz, CD_3CN) spectrum of complex **6**.

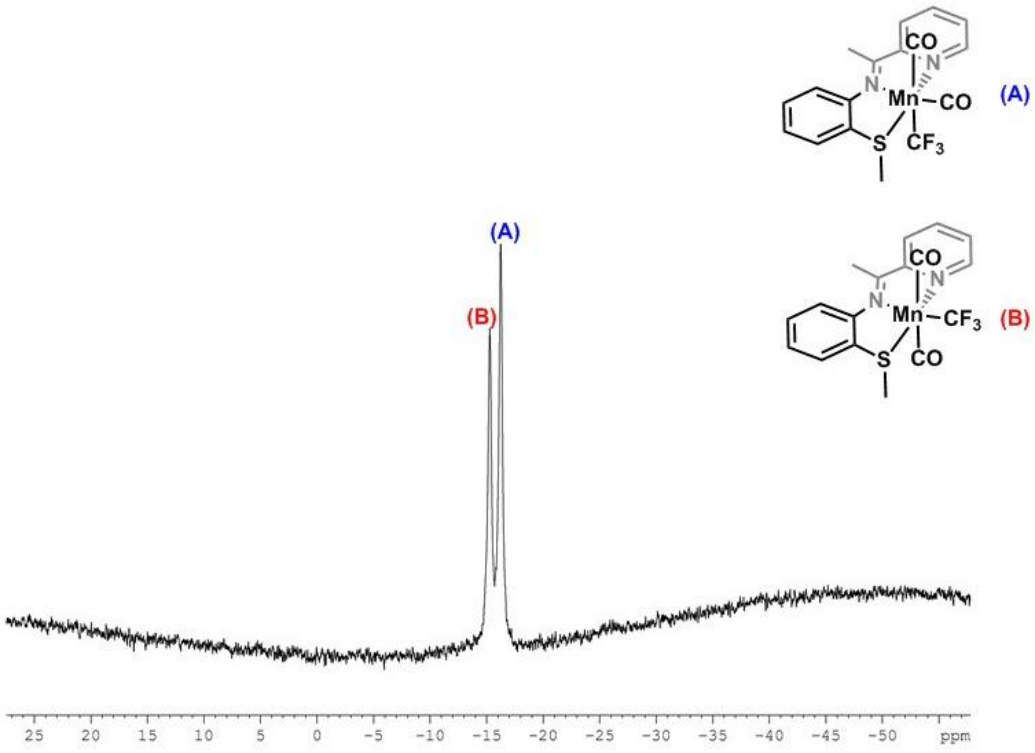

Figure S11: ^{19}F NMR (282 Mhz, CD_3CN) of complex 7.

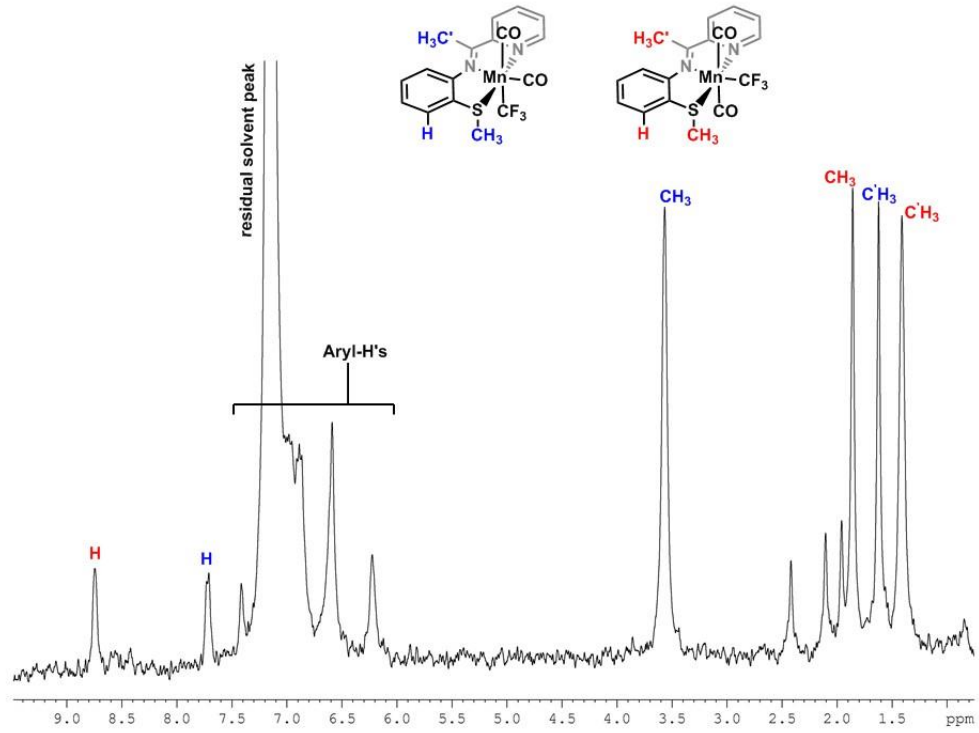

Figure S12: ^{1}H NMR (300 MHz, CD_3CN) spectrum of complex **7**.

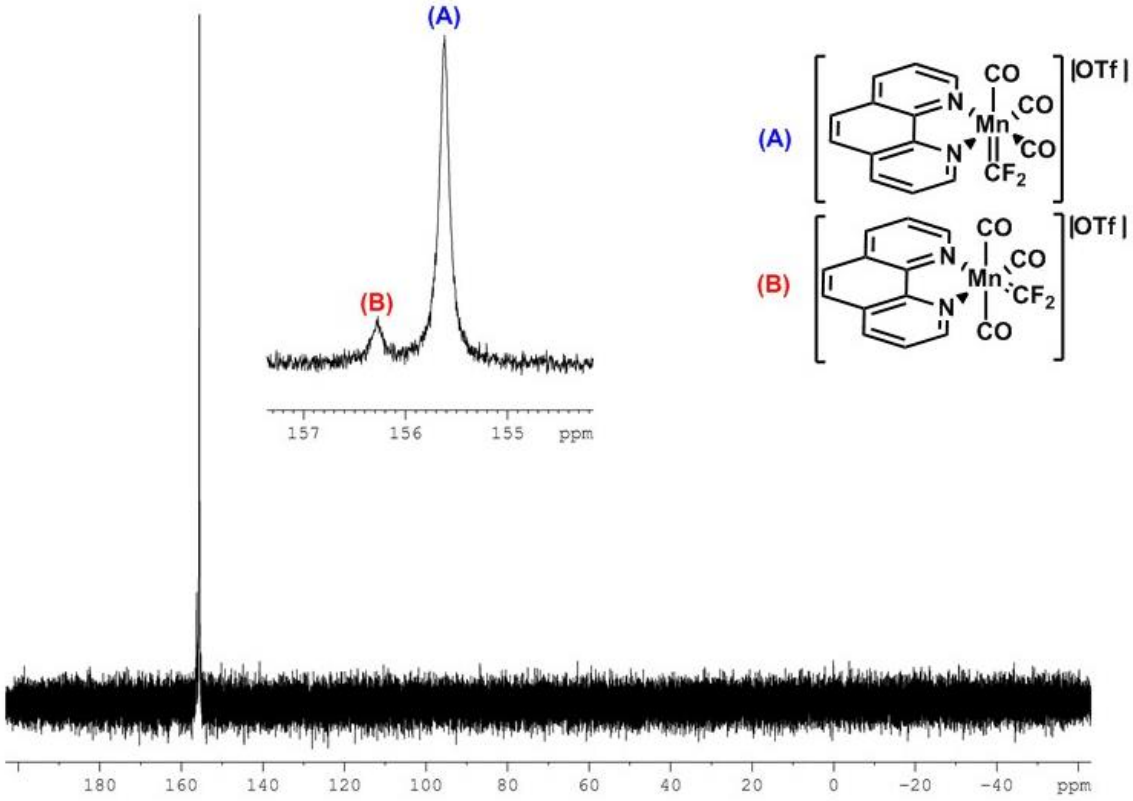

Figure S13: ^{19}F NMR (282 Mhz, C_6D_6) downfield spectrum of complex **8**.

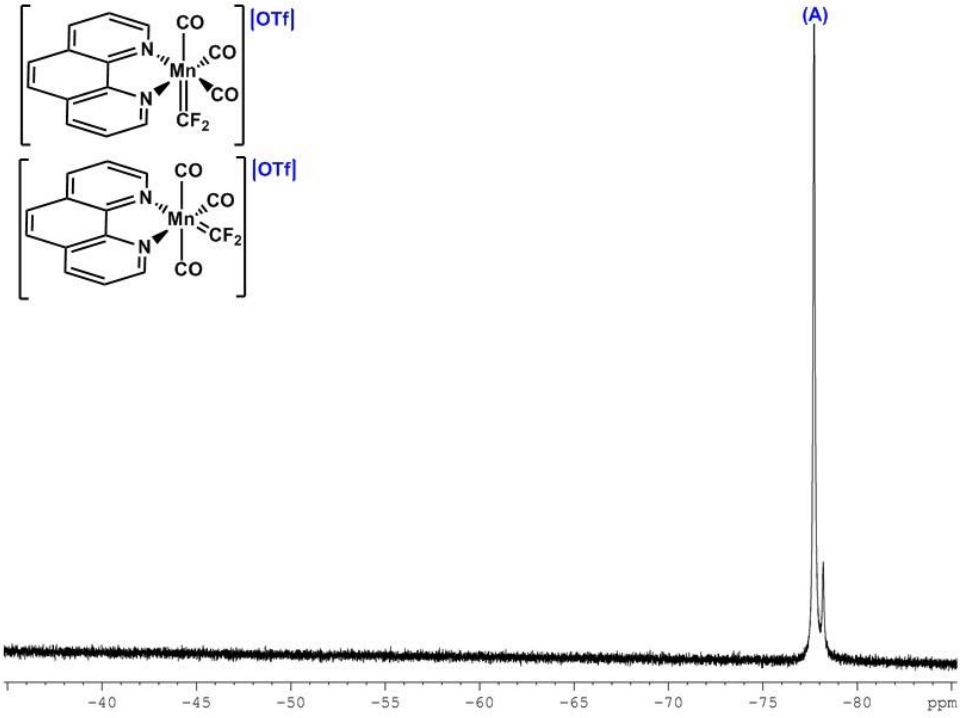

Figure S14: ^{19}F NMR (282 Mhz, C_6D_6) upfield spectrum of complex **8**.

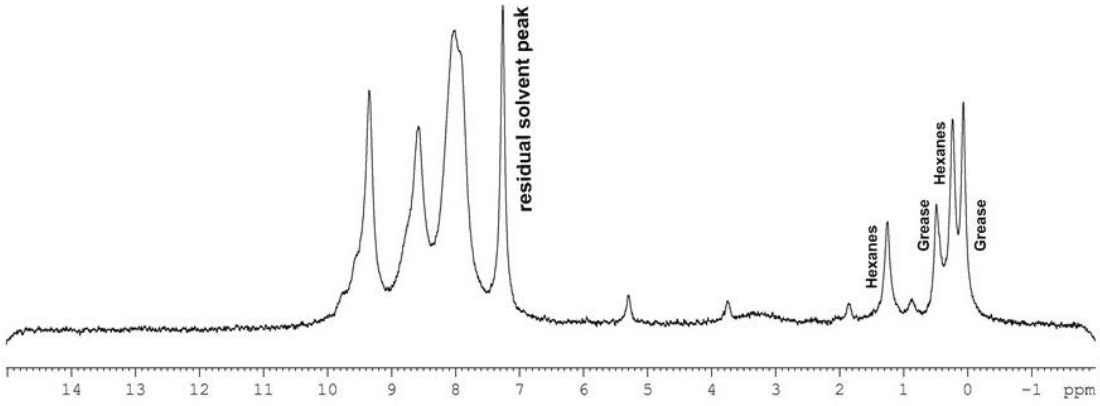

Figure S15: ^{1}H NMR (300 MHz, $CDCl_3$) spectrum of complex **8**.

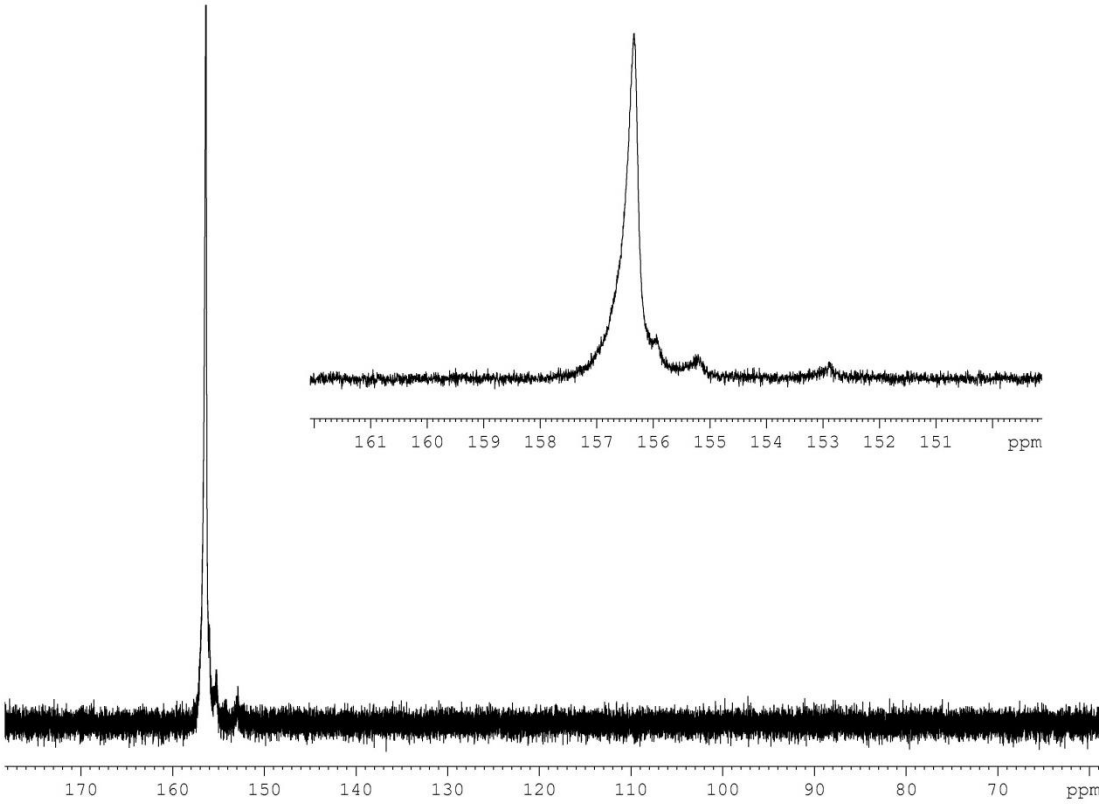

Figure S16: ^{19}F NMR (282 MHz, C_6D_6) downfield spectrum of $(NNS)(CO)_2Mn{=}CF_2$ complex.

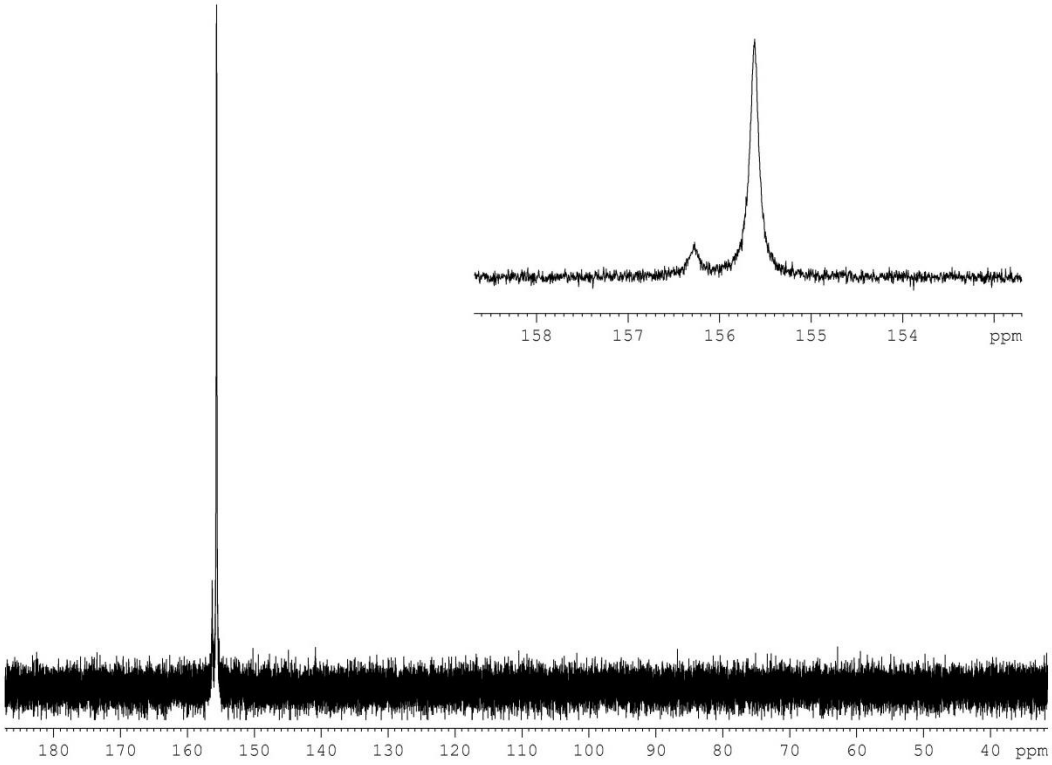

Figure S17: ^{19}F NMR (282 MHz, C_6D_6) downfield spectrum of $(Bpy)(CO)_3Mn{=}CF_2$ complex. Minor peak at 156.3 is proposed to be an isomeric $Mn{=}CF_2$ complex.

Cyclic Voltammetry Data:

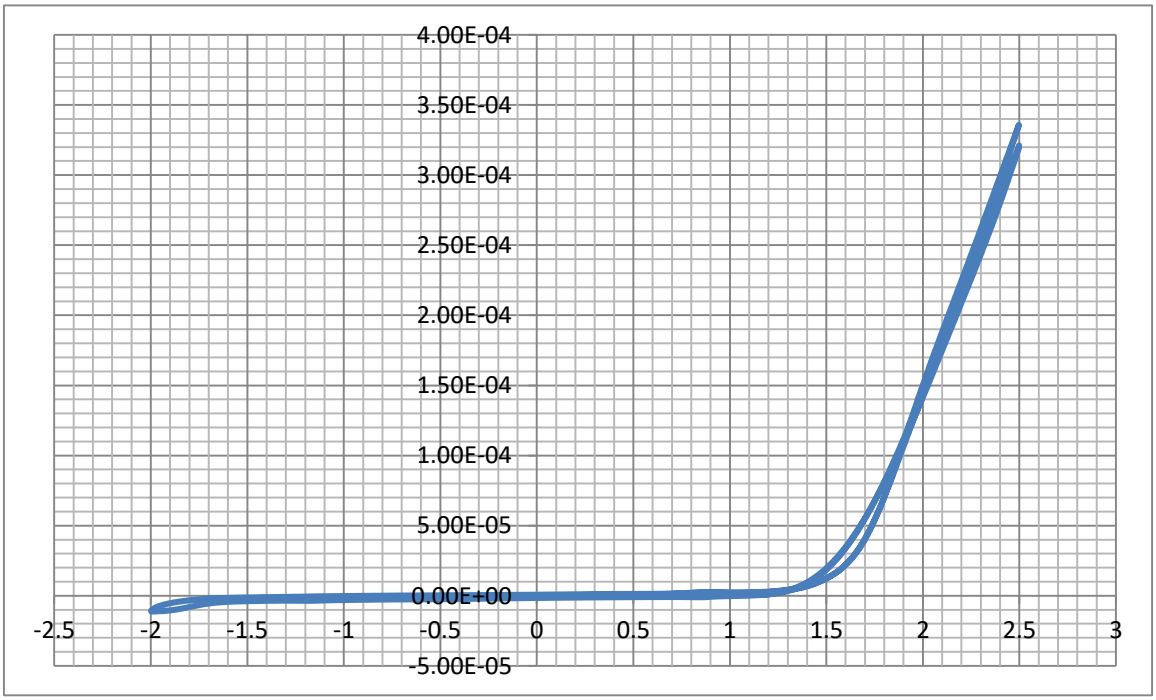

Figure S18: Blank Cyclic Voltammogram (0.1M THF solution of $[(Bu)_4N][BF_4]$)

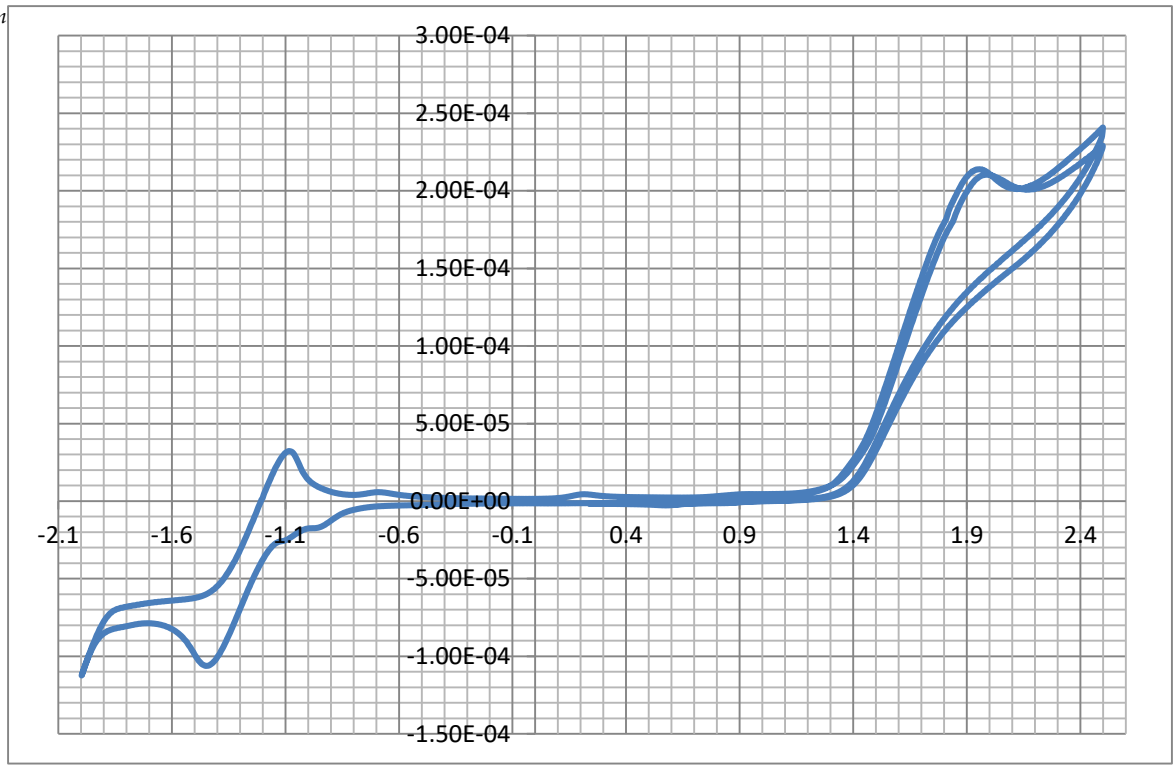

Figure S19: Cyclic Voltammogram of complex **3** in THF (100mV/s sweep rate) showing irreversible oxidation at approx. 0.6 V vs. ferrocene and quasi-reversible reduction at -2.3 V vs. ferrocene

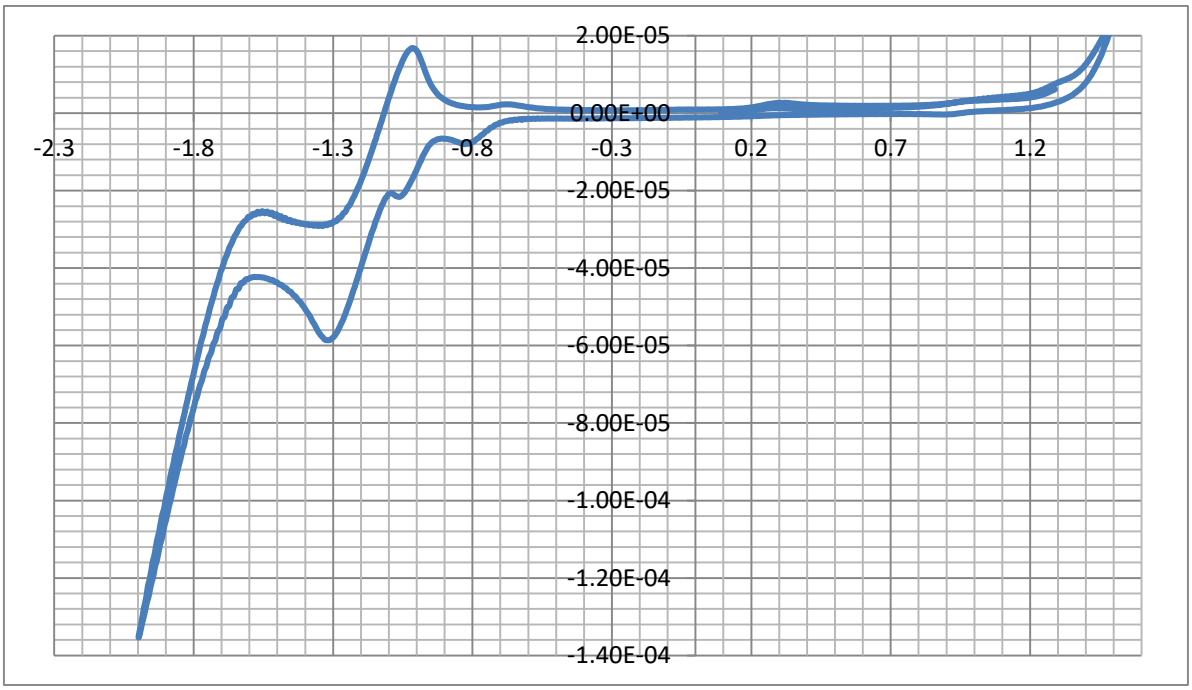

Figure S20: Cyclic Voltammogram of -0.5V - +1.5V region of complex 4 in THF (100mV/s sweep rate) showing quasi-reversible reduction at -2.1 V vs. ferrocene

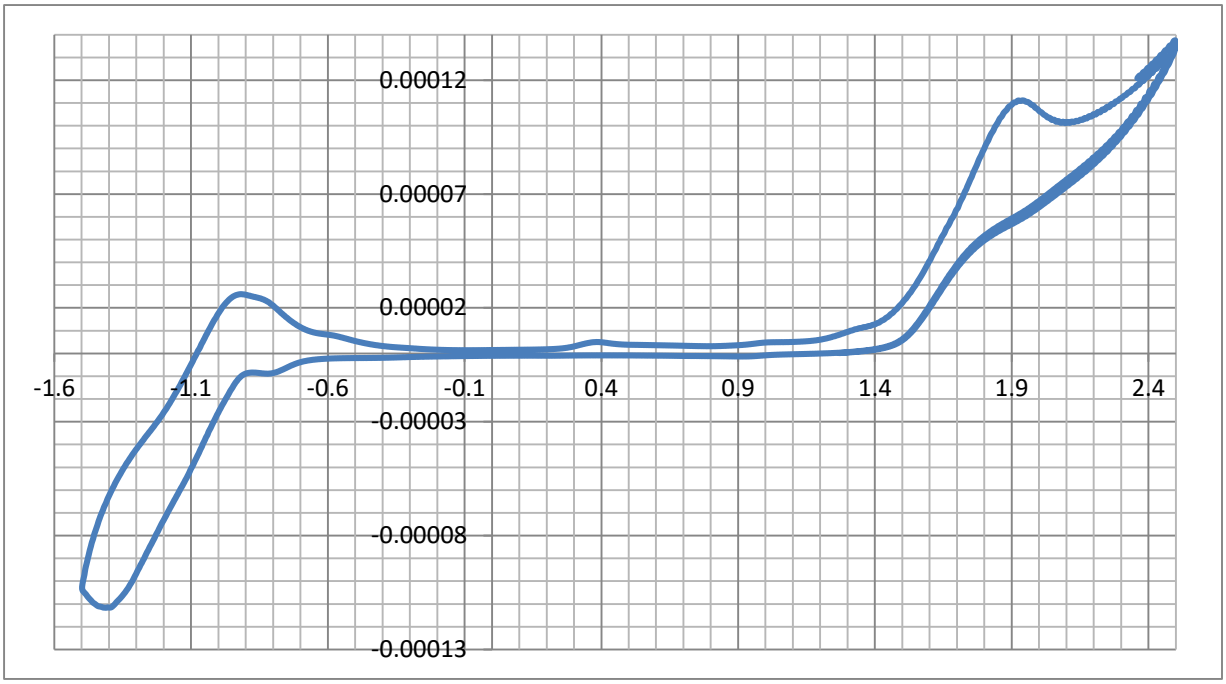

Figure S21: Cyclic voltammogram of -1.5 - 2.5 V region for complex **4** in THF (100mV/s sweep rate) showing non-reversible oxidation at 0.66V vs ferrocene

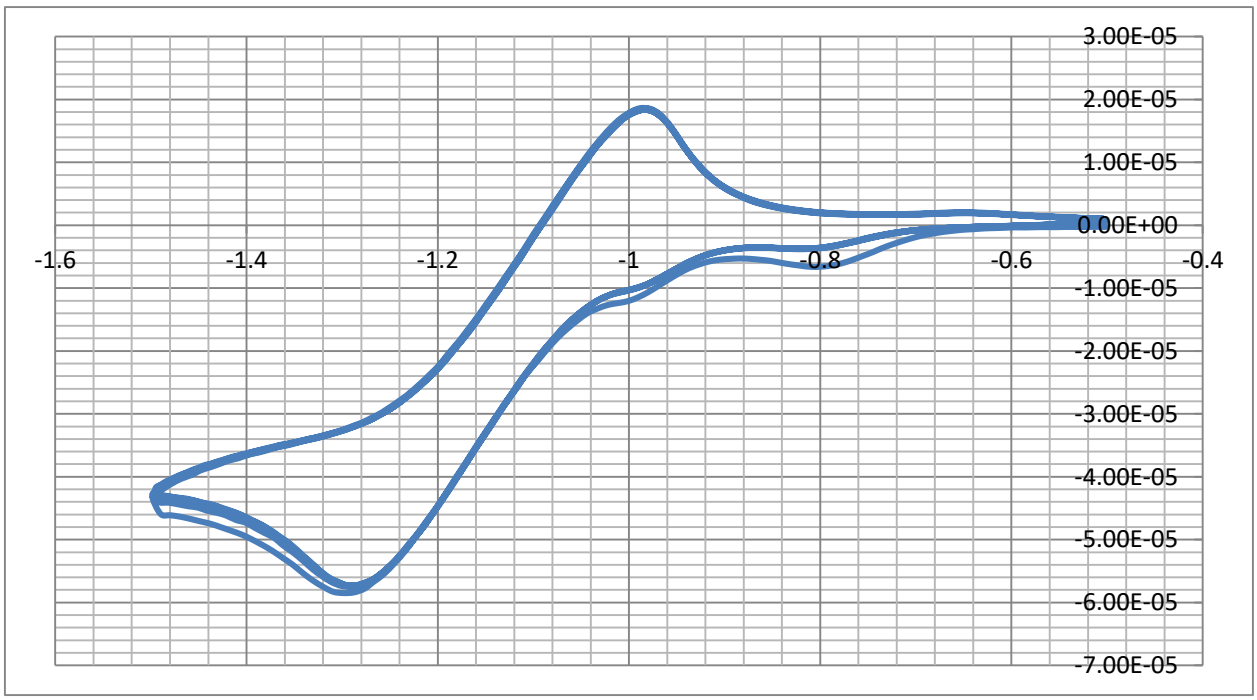

Figure S22: Cyclic voltammogram of -0.5V - -1.5V region for complex **4** in THF (100 mV/s sweep rate) showing possible irreversible oxidation and quasi-reversible reduction

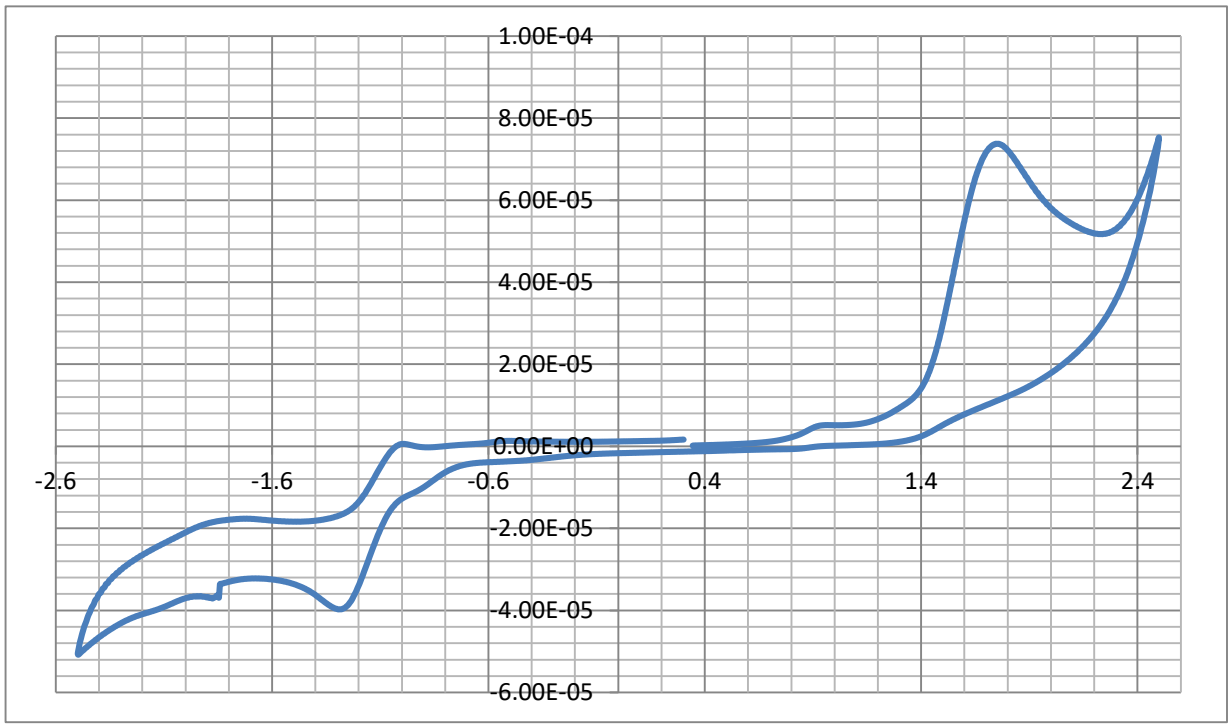

Figure S23: Cyclic voltammogram of complex7 in THF (100 mV/s sweep rate) showing possible irreversible oxidation and quasi-reversible reduction

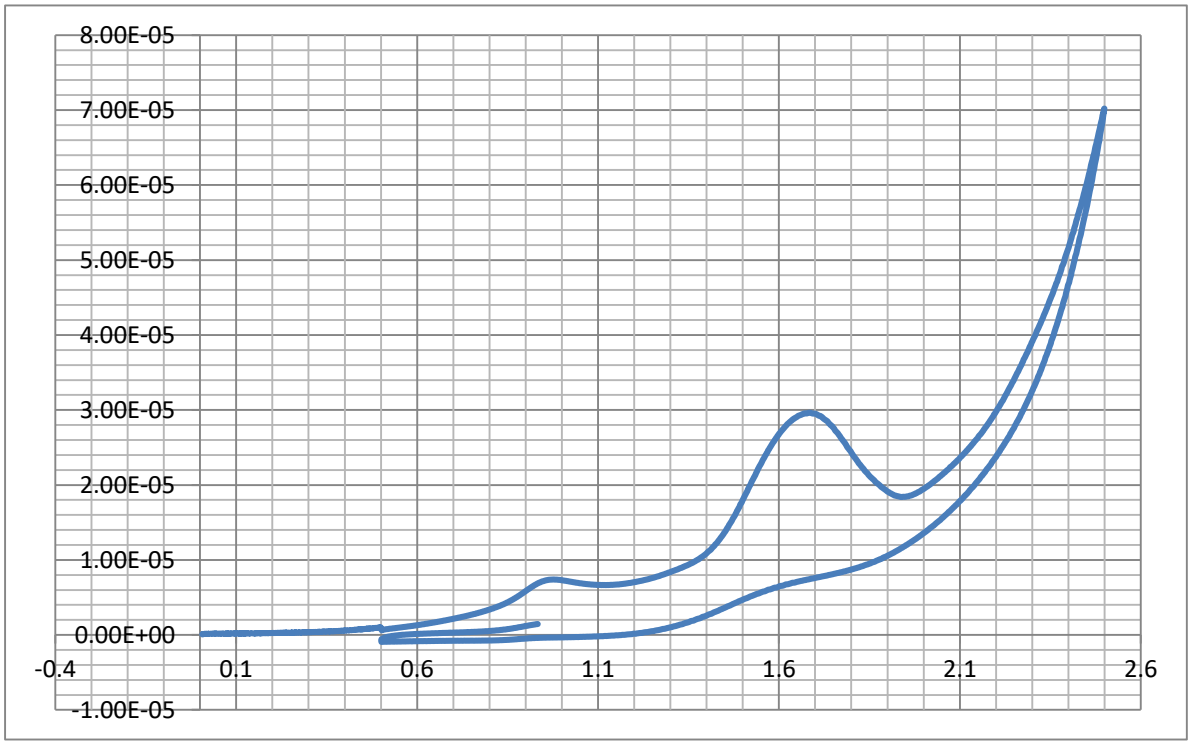

Figure S24: Cyclic voltammogram of complex**7** in THF (100 mV/s sweep rate) showing possible irreversible oxidation and quasi-reversible reduction

EI-MS Data:

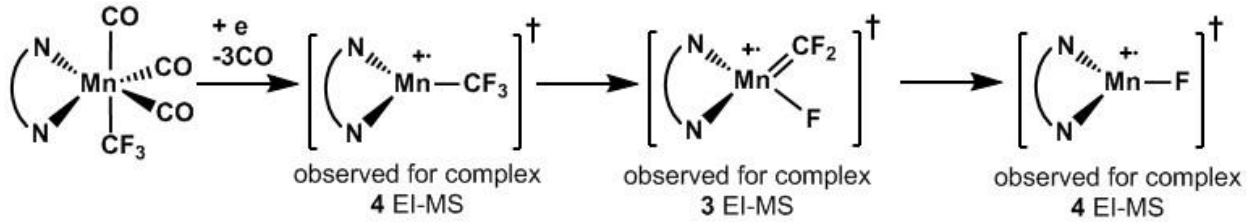

Figure S25: Hypothetical fragmentation of complex **3** and **4** after electron impact (EI)

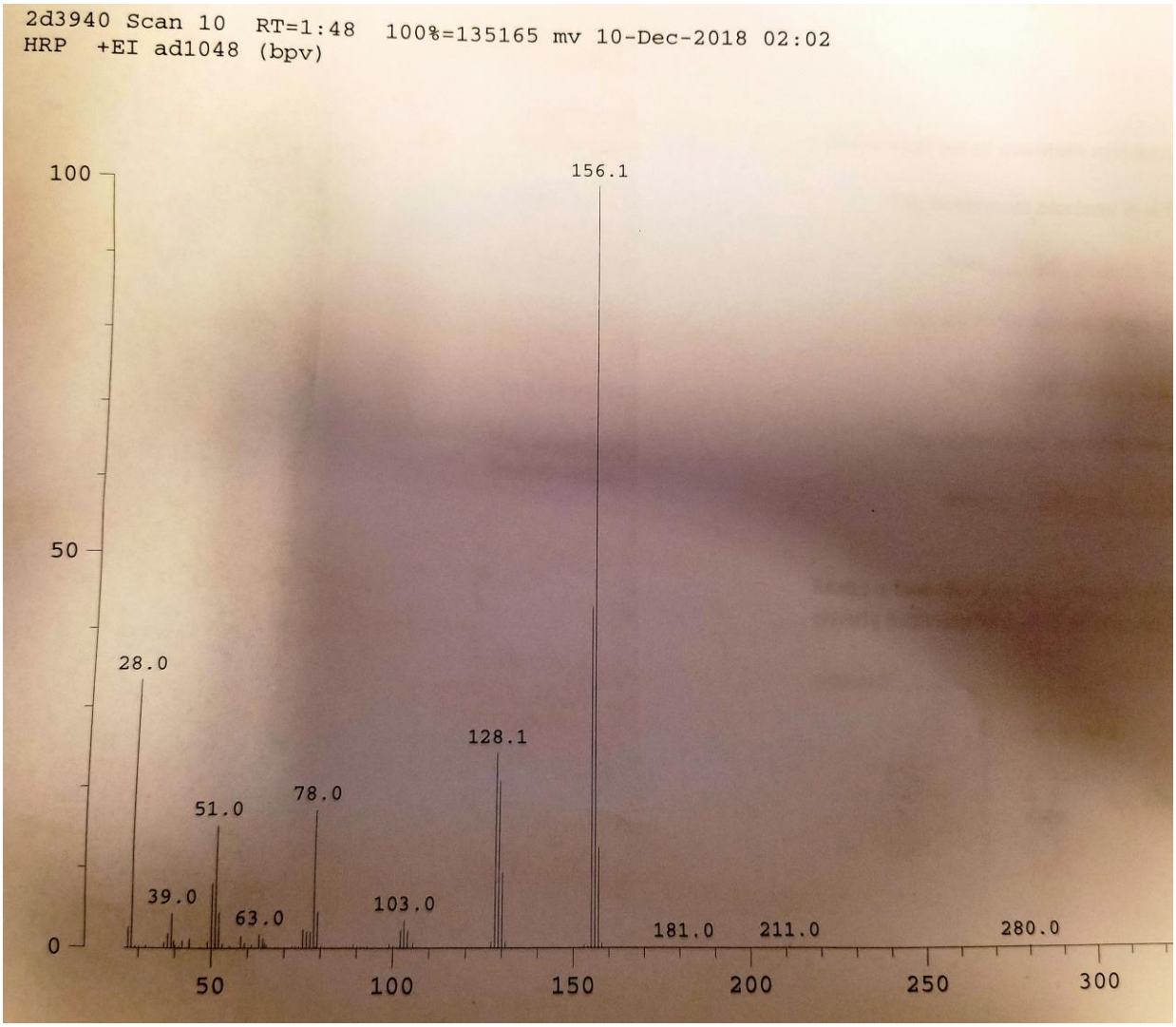

Figure S26: EI-MS spectrum of fragmentation of complex **3** showing $N_2(F)Mn{=}CF_2$ fragment.

Formula search on scan 10 of 2d3940

Mass	Int%	Dev mmu	1 H	12 C	14 N	19 F	55 Mn
280.00375	0.20	-2.39	0	21	2	0	0
		-8.70	2	20	0	2	0
		3.87	0	19	1	2	0
		-8.50	1	15	3	3	0
		-4.77	9	18	0	0	1
		7.80	7	17	1	0	1
		-4.57	8	13	3	1	1
		8.00	6	12	4	1	1
		1.69	8	11	2	3	1

Figure S27: Exact mass search for $N_2(F)Mn{=}CF_2$ (N_2 = Bipy) of mass 280.00375 Da

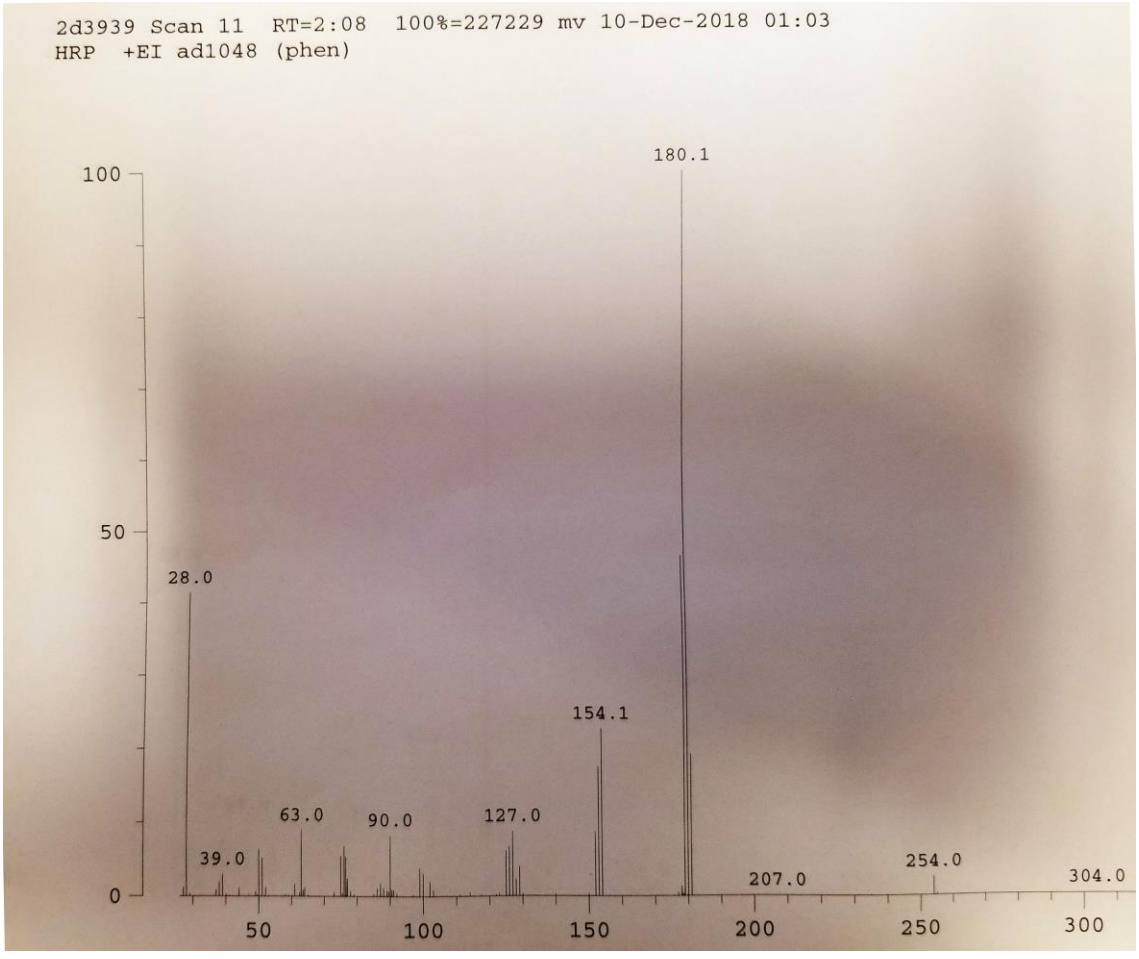

Figure S28: EI-MS for complex **4** showing $N_2Mn\text{-}CF_3$ and $N_2Mn\text{-}F$ fragments (304.0 and 254Da respectively)

Formula search on scan 11 of 2d3939

Mass	Int%	Dev mmu	1 H	12 C	14 N	19 F	55 Mn
303.99905	0.09	-7.09	0	23	2	0	0
		-0.83	0	21	1	2	0
		-9.47	9	20	0	0	1
		3.10	7	19	1	0	1
		-9.27	8	15	3	1	1
		3.30	6	14	4	1	1
		9.37	7	17	0	2	1
		-3.01	8	13	2	3	1
		9.57	6	12	3	3	1

Figure S29: Exact mass for $N_2Mn\text{-}CF_3$ (N_2 = Phen) exact mass of 303.99905 Da

Formula search on scan 11 of 2d3939

Mass	Int%	Dev mmu	1 H	12 C	14 N	19 F	55 Mn
254.00625	2.55	-9.40	2	21	0	0	0
		3.17	0	20	1	0	0
		-9.20	1	16	3	1	0
		9.44	0	18	0	2	0
		-2.94	1	14	2	3	0
		0.99	8	12	2	1	1
		-5.31	10	11	0	3	1
		7.26	8	10	1	3	1

Figure S30: Exact mass of $N_2Mn\text{-}F$ (N_2 = Phen) exact mass of 254.00625 Da